Atmospheric Trace Gas Measurements from the European Space Agency's Global Ozone Monitoring Experiment

K. Chance, R.J.D. Spurr, and T.P. Kurosu

Harvard-Smithsonian Center for Astrophysics
60 Garden Street, Cambridge, MA 02138 USA

ABSTRACT

The Global Ozone Monitoring Experiment (GOME) was launched on the European Space Agency's ERS-2 satellite on April 20, 1995. GOME measures the Earth's atmosphere in the nadir geometry, using four spectrometers that cover the UV and visible (238-794 nm) at moderate resolution (0.2 nm in the UV, 0.4 nm in the visible), employing silicon diode array detectors. GOME takes some 30,000 spectra per day, obtaining full global coverage at 40×320 km^2 resolution in three days. It provides measurements of ozone (including the tropospheric distribution), NO_2, SO_2, H_2CO, H_2O, BrO, ClO, and OClO. We directly fit GOME radiance spectra using nonlinear least-squares analysis to obtain column amounts of several trace species, including ClO, BrO, SO_2, and H_2CO. The use of recent improvements in the underlying physics and spectroscopy permits the fitting of radiances to very high precision, approaching 2×10^{-4} (optical thickness) in favorable cases, for standard 1.5 s integration time GOME measurements. Examples of the fitting of BrO and SO_2 are presented here.

Keywords: Remote sensing, GOME, stratosphere, troposphere

1. DEVELOPMENT OF FITTING TECHNIQUE

The GOME instrument was designed to make sensitive measurements of a number of atmospheric constituents, including ozone (column amounts and profiles, including the tropospheric burden), NO_2, SO_2, H_2CO, H_2O, BrO, ClO, and OClO.[1,2] GOME provides spectra that are stable in behavior and reasonably well-calibrated in wavelength (usually to $\leq6\times10^{-3}$ nm or ≤0.05 GOME pixel in the BrO fitting region, for example) and absolute radiance. They provide an ideal data set for exploring both geographic and temporal variations for a number of atmospheric constituents.

In order to fully exploit the GOME data products for these purposes, we have found it necessary to further calibrate and characterize the GOME irradiance and radiance spectra and the reference spectra used for fitting to determine constituent amounts. This includes: (1) Improved wavelength calibration of both irradiance and radiance spectra, which is accomplished either by cross-correlation with or direct fitting to a very accurate Fraunhofer reference spectrum.[3,4] Absolute vacuum wavelength calibration can be obtained by these methods to usually ±0.001 nm or better; (2) Improved determination of the GOME instrument transfer function (ITF).[4] In the BrO fitting region, the width of the ITF is determined to the 1% level. In some other regions, determination can be more problematic, since the ITF can vary substantially with wavelength near the endpoints of the GOME spectral channels (SO_2 fitting is done in such a region, for example); (3) Improved determination of the correction for the inelastic component of atmospheric molecular scattering (the "Ring effect"). The primary component of the Ring effect for the GOME viewing geometry is rotational Raman scattering. We have performed a comprehensive study of the molecular physics of the rotational Raman scattering in the atmosphere, including the use of the best available values for the wavelength-dependent polarizabilities and their anisotropies for N_2 and O_2, the full quantum and statistical mechanics of Raman scattering (including the contribution from the triplet structure of the $^3\Sigma_g^-$ O_2 ground

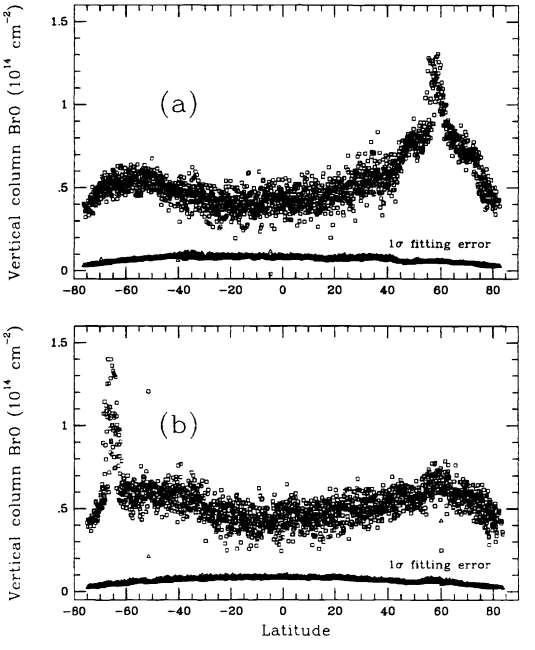

Figure 1. Enhanced tropospheric BrO in Arctic (a) and Antarctic spring (b).

Part of the EUROPTO Conference on Satellite Remote Sensing of Clouds and the Atmosphere III • Barcelona, Spain • September 1998
SPIE Vol. 3495 • 0277-786X/98/$10.00

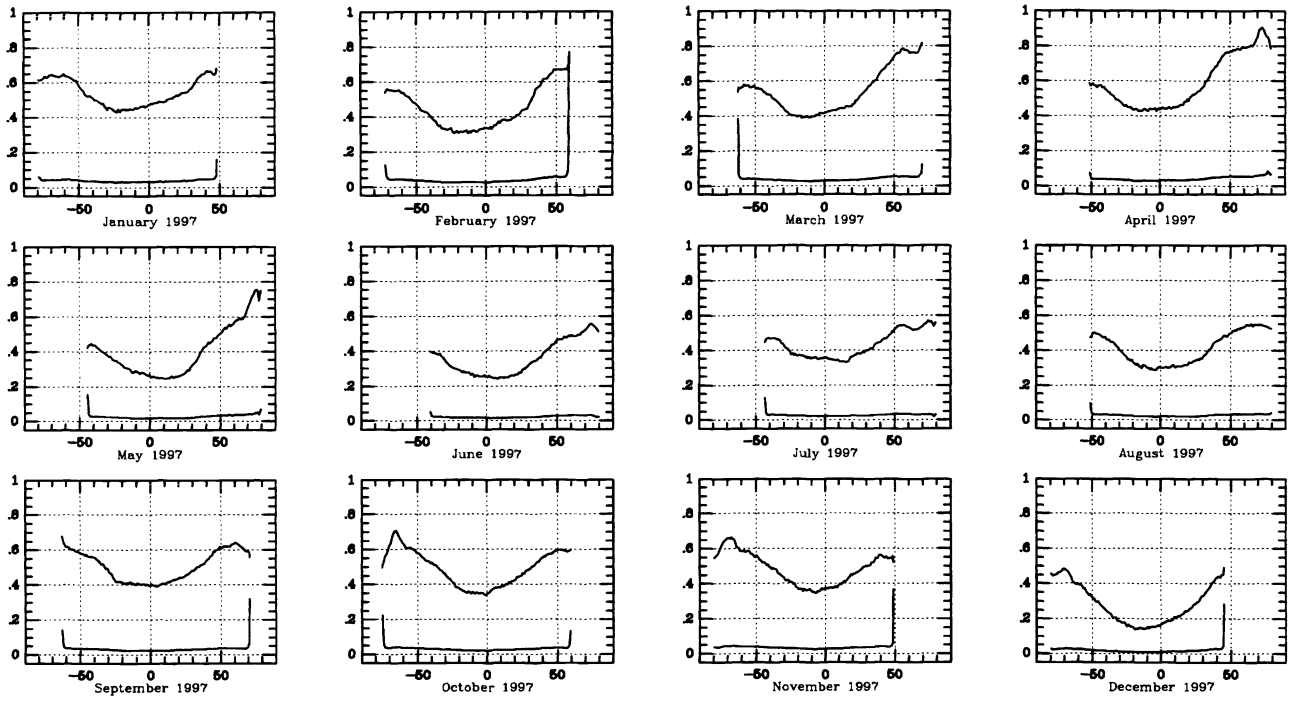

Figure 2. Vertical column BrO (10^{14} cm^{-2}) vs. latitude, including 1σ fitting errors.

state), and the interaction with an accurate Fraunhofer reference spectrum.[5] This provides us with best available Ring effect corrections for atmospheric measurements over the GOME range. The corrections include wavelength-dependent cross sections, phase functions, and all polarization dependence. The spectral structures for interference between Ring effect scattering and molecular absorption are readily calculated to first order in scattering by multiplying the appropriate absorption cross sections and rotational Raman cross sections together before convolution with the Fraunhofer reference spectrum; (4) Correction for undersampling in the GOME spectra. We determined that the large systematic residuals in the fitting of GOME spectra are almost entirely due to undersampling of the ITF by the GOME detector arrays (aliased into both irradiance and radiance spectra and showing up in the difference because of the slightly different ITFs for irradiance and radiance measurements). Using the Fraunhofer reference spectrum[5] and the ITF determined by fitting GOME irradiance to determine the wavelength calibration, we have determined a method for correcting for more than 90% of this residual in favorable parts of the spectrum by re-sampling over- and under-sampled representations of the Fraunhofer reference spectrum;[4] (5) Improvements to reference spectra. In particular, some of the reference spectra commonly used for fitting are not accurately calibrated in wavelength, and can suffer from the use of air wavelength scales which do not include sufficient reference to the appropriate conversion to vacuum wavelength. We are involved in work to develop improved databases of reference spectra, which includes accurate vacuum-wavelength calibration. To date we have performed re-calibrations for the reference spectra needed to fit BrO, SO_2, and H_2CO. Improved wavelength calibration for O_3 and NO_2 is underway.

GOME spectra are directly fitted by a standard nonlinear least-squares method,[6,7] with all of the above improvements fully included. A fitting window is selected and a radiance spectrum calculated and adjusted by iteration until it agrees with the measured spectrum in the least-squares sense to within preset convergence criteria. Because of the generally good quality of the GOME spectra and the substantial groundwork in the molecular physics, calibration, and characterization that we have performed for the quantitative fitting, we are able to determine trace gas amounts with quite high precision without the need to high-pass filter the spectra to remove baseline anomalies. We do not need to smooth the measured and reference spectra in order to reduce the apparent residuals, nor is it necessary to "shift" and "squeeze" the wavelength scales of the reference spectra in order to correct for inaccuracies in wavelength calibration. In direct intercomparisons among GOME investigators, application of the method and the reference data described here gives an order of magnitude improvement for the precisions of trace gas amounts obtained from GOME spectra in comparison with results from other fitting methods.

2. FITTING AND ANALYSIS OF BRO

The fitting procedure for BrO is now mature. BrO is routinely fitted over the 344-359 nm region. Cross sections for BrO, O_3, NO_2, OClO, and the O_2-O_2 collision complex, and the reference spectrum for the Ring effect are included in the fitting. The window containing BrO is fitted to typically 3-4 $\times 10^{-4}$ RMS optical thickness, for single, non-smoothed 1.5 s integration time level 1 spectra, providing slant column uncertainties of ca. 10^{13} cm^{-2} (usually 4-20%).

In order to determine vertical column amounts of BrO from the measured slant columns, it is necessary to determine "air mass factors" correcting the measurement geometry for atmospheric scattering processes and penetration depth. For BrO located at 15 km and above, where solar zenith angles (SZAs) are $\leq 70°$, and the albedo is 0.1 or greater, the use of geometric air mass factors is determined by radiative transfer calculations to be accurate to better than 10%. For the present work, geometric air mass factors are used. For the largest SZAs measured by GOME, the tropospheric column will be under-determined by up to a factor of two in this approximation. This is mainly of importance in polar regions in the spring, where there are substantial enhancements in BrO that are almost certainly tropospheric.[4,8] We are currently working to fully parameterize the air mass factors for the range of BrO distributions, SZAs, and albedos measured by GOME.

Events of localized springtime production of BrO are readily seen, and the increase in the polar vortex can be monitored well.[4,8] Figure 1a shows an example of the enhancement of column BrO over Hudson Bay, Canada on September 15, 1996, while Figure 1b shows an example of such enhancement in the Antarctic, over the Amery Ice Shelf on March 21, 1997.

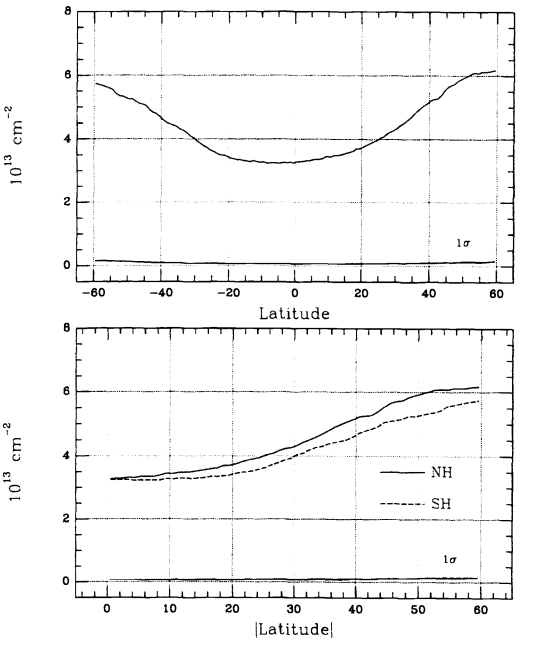

Figure 3. Vertical column BrO vs. latitude; whole range (top) and southern and northern hemisphere overlaid (bottom).

2.1. Preliminary BrO climatology studies

Research is currently underway in our institution to determine the climatology of BrO on a more global basis. We have analyzed GOME level 1 data from 1997 for BrO by selecting 16 CD-ROMs (each CD-ROM usually contains 35 ERS-2 orbits, about 2.5 days of GOME observations). One CD-ROM for each month of 1997, plus the last two months of 1996 and the first two months of 1998, was chosen. Each CD-ROM includes the 21st day of that particular month. BrO is fitted for all orbits on each of the CDs selected. Orbits where the data are adversely affected by the South Atlantic Anomaly (evident from extremely noisy spectra and poor fitting results for BrO as well as other species) are then excluded from further statistical studies, leaving 14-24 orbits from each CD in the analysis. Data are further selected to include only results from spectra taken at SZAs of 70° or less. This is to ensure that the use of geometrical air mass factors for stratospheric BrO vertical column determination is a reasonable approximation. Weighted averages of the fitting results for each month are made over 1° latitude bins. The resulting determinations of vertical column BrO versus latitude, and their uncertainties, are shown in Figure 2. The varying coverage over the year is due to the seasonal variation of SZA versus latitude. An average for the full year (including 275,096 individual GOME spectra) for the column BrO up to ±60° latitude is shown in Figure 3 (top). Figure 3 (bottom) shows the same data, but plotted with the northern and southern hemispheres overlaid, as a first comparison of possible interhemispheric differences. An area-weighted ratio of northern hemisphere to southern hemisphere BrO can be taken over the limits ±40° in latitude, the range for which all months include data at SZA $\leq 70°$. The result is 1.074±0.032 (1σ). However, the spread in results for individual months (plotted in Figure 4) indicates that there is too much variation for the overall yearly-averaged ratio to have much statistical meaning.

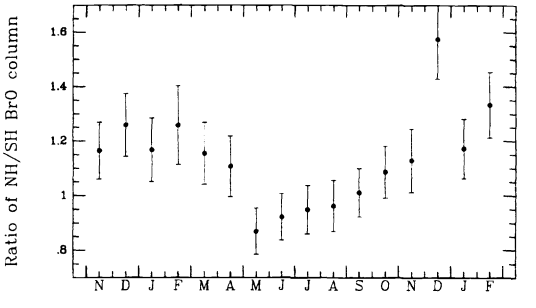

Figure 4. Temporal variation of 1997 NH/SH BrO column up to 40°.

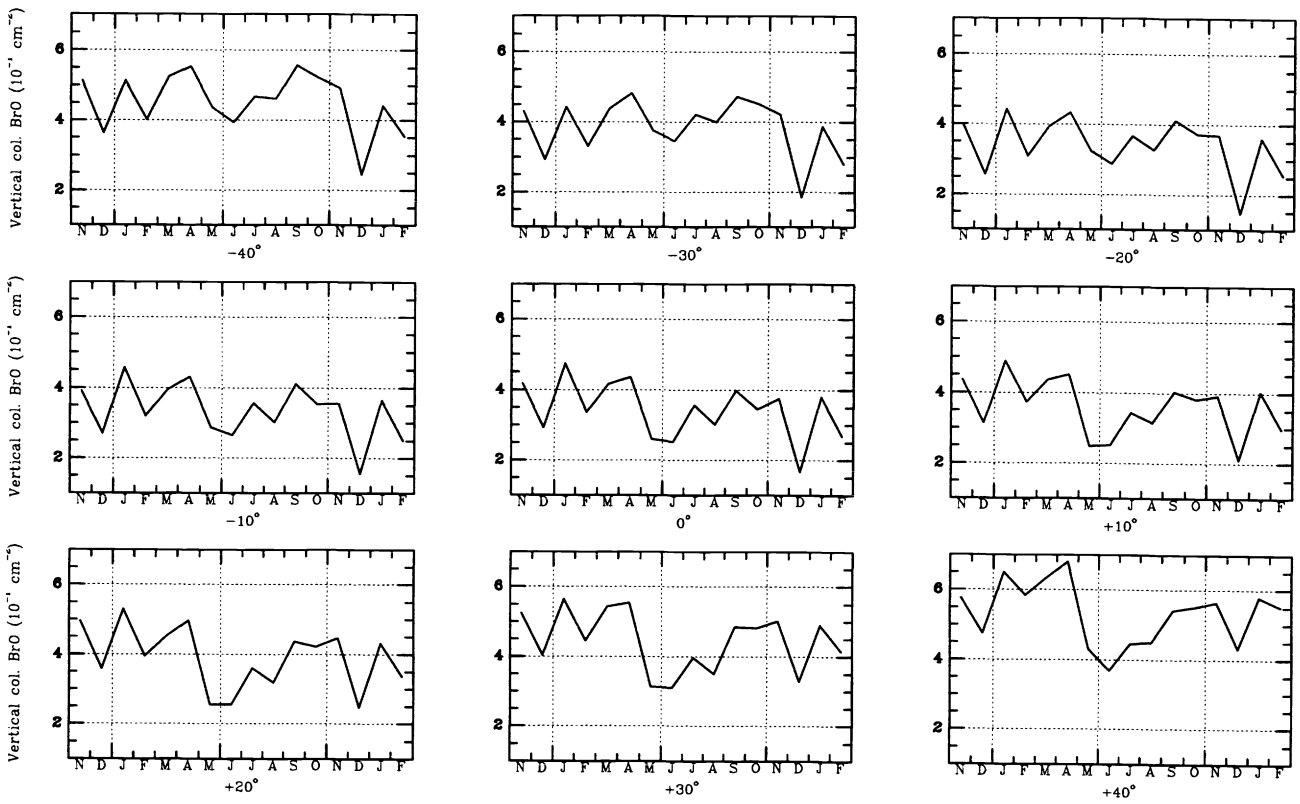

Figure 5. Temporal variation of 1997 BrO column at different latitudes.

We have also determined the temporal variation of column BrO for different latitudes from −40 to +40°, shown in Figure 5. An overall yearly phase structure is apparent at all latitudes, with column BrO peaking in the spring and fall. The smaller-scale structure which is evident for the different latitudes may be an artifact due to the analysis of only a limited number of orbits for each time period; how much of this structure is real is an area of current research.

2.2. Tropospheric BrO

An additional preliminary study is concerned with the proportion of BrO in low- and mid-latitudes that may lie in the troposphere. It has been suggested that there might be a non-negligible tropospheric BrO background (T. Wagner, K. Pfeilsticker, and U. Platt, University of Heidelberg). We have made correlation studies between BrO columns and GOME cloud coverage from the GOME Initial Cloud Fitting Algorithm for seven orbits over the mid-Pacific during October, 1997 (cloud-top heights of 400-600 mbar). The orbits were chosen over the ocean, in order to simplify considerations of albedo versus cloud coverage; they were further selected to have highly variable cloud coverage. The result of correlating column BrO and cloud coverage is corrected for air mass factors due to tropospheric BrO using standard radiative transfer calculation techniques. The tropospheric BrO background mixing ratio below cloud-top height over the range of latitudes covered (approximately ±50°) is determined to be 0.3 pptv or less.

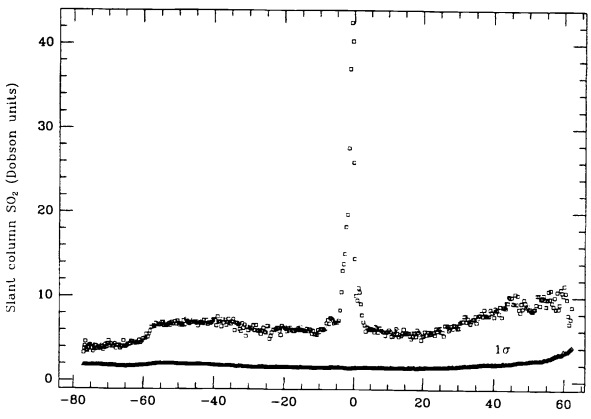

Figure 6. GOME orbit 61204081: SO_2 vs. latitude (Mt. Nyamuragira).

3. FITTING AND ANALYSIS OF SO_2

SO_2 fitting is less mature, but is improving rapidly. Fitting uncertainties are typically 2×10^{-3} optical thickness (RMS); slant column uncertainties are ca. 2 Dobson units. A factor of 4-5 improvement is anticipated in the near term from improvements in the spectroscopic data base and further characterization of the GOME instrument. The current level of fitting does provide for precise measurement of volcanic plumes, and may provide measurements of SO_2 background levels, industrial pollution, and the behavior of SO_2 in the polar vortex. Figure 6 is an example of SO_2 fitting, for an orbit whose observation includes the active volcano Mount Nyamuragira, Zaire (Democratic Republic of Congo). For comparison with previous fitting results, see *Eisinger* et al., *1997*.[9] In addition to the enhanced SO_2 from the volcano, there is evidence of tropospheric pollution over Western Siberia and a shelf in the SO_2 concentration coincident with the remnant of the 1996 Antarctic ozone hole. Whether these smaller features are truly variations in SO_2 or are artifacts of the fitting process is currently under investigation.

ACKNOWLEDGMENTS

We thank the European Space Agency and the DLR-DFD for cooperation that has been essential to this work. This research was supported by NASA Grant NAG5-3461.

REFERENCES

1. K. Chance, J. Burrows, and W. Schneider, "Retrieval and Molecule Sensitivity Studies for the Global Ozone Monitoring Experiment and the SCanning Imaging Absorption spectroMeter for Atmospheric CHartographY," in *Proceedings S.P.I.E., Remote Sensing of Atmospheric Chemistry*, vol. 1491, pp. 151–165, 1991.
2. J. Burrows, K. Chance, A. Goede, R. Guzzi, B. Kerridge, C. Muller, D. Perner, U. Platt, J.-P. Pommereau, W. Schneider, R. Spurr, and H. van der Woerd, "Global Ozone Monitoring Experiment Interim Science Report, ed. T.D. Guyenne and C. Readings," Tech. Rep. Report ESA SP-1151, ISBN 92-9092-041-6, ESA Publications Division, ESTEC, Noordwijk, The Netherlands, 1993.
3. C. Caspar and K. Chance, "GOME Wavelength Calibration Using Solar and Atmospheric Spectra," in *Proc. Third ERS Symposium on Space at the Service of our Environment, European Space Agency publication SP-414, ISBN 92-9092-656-2*, T.-D. Guyenne and D. Danesy, eds., pp. 609–614, 1997.
4. K. Chance, "Analysis of BrO Measurements from the Global Ozone Monitoring Experiment," *Geophysical Research Letters* **25**(17), pp. 3335–3338, 1998.
5. K. Chance and R. Spurr, "Ring Effect Studies: Rayleigh Scattering, Including Molecular Parameters for Rotational Raman Scattering, and the Fraunhofer Spectrum," *Applied Optics* **36**, pp. 5224–5230, 1997.
6. D. Marquardt, "An Algorithm for Least-Squares Estimation of Non-Linear Parameters," *J. Soc. Indust. Appl. Math.* **2**, pp. 431–441, 1963.
7. W. Press, B. Flannery, S. Teukolsky, and W. Vetterling, *Numerical Recipes, ISBN 0-521-30811-9*, Cambridge University Press, 1986.
8. A. Richter, F. Wittrock, M. Eisinger, and J. Burrows, "GOME Observations of Tropospheric BrO in Northern Hemisphere Spring and Summer 1997," *Geophysical Research Letters* **25**, pp. 2683–2686, 1998.
9. M. Eisinger, J. Burrows, A. Richter, and A. Ladstätter-Weißenmeyer, "SO_2, OClO, BrO, and Other Minor Trace Gases from the Global Ozone Monitoring Experiment (GOME)," in *Proc. Third ERS Symposium on Space at the Service of our Environment, European Space Agency publication SP-414, ISBN 92-9092-656-2*, T.-D. Guyenne and D. Danesy, eds., pp. 675–680, 1997.